

THE OFFICIAL MAGAZINE OF THE OCEANOGRAPHY SOCIETY

# Oceanography

CITATION

Simmons, H., M.-H. Chang, Y.-T. Chang, S.-Y. Chao, O. Fringer, C.R. Jackson, and D.S. Ko. 2011. Modeling and prediction of internal waves in the South China Sea. *Oceanography* 24(4):88–99, <http://dx.doi.org/10.5670/oceanog.2011.97>.

DOI

<http://dx.doi.org/10.5670/oceanog.2011.97>

COPYRIGHT

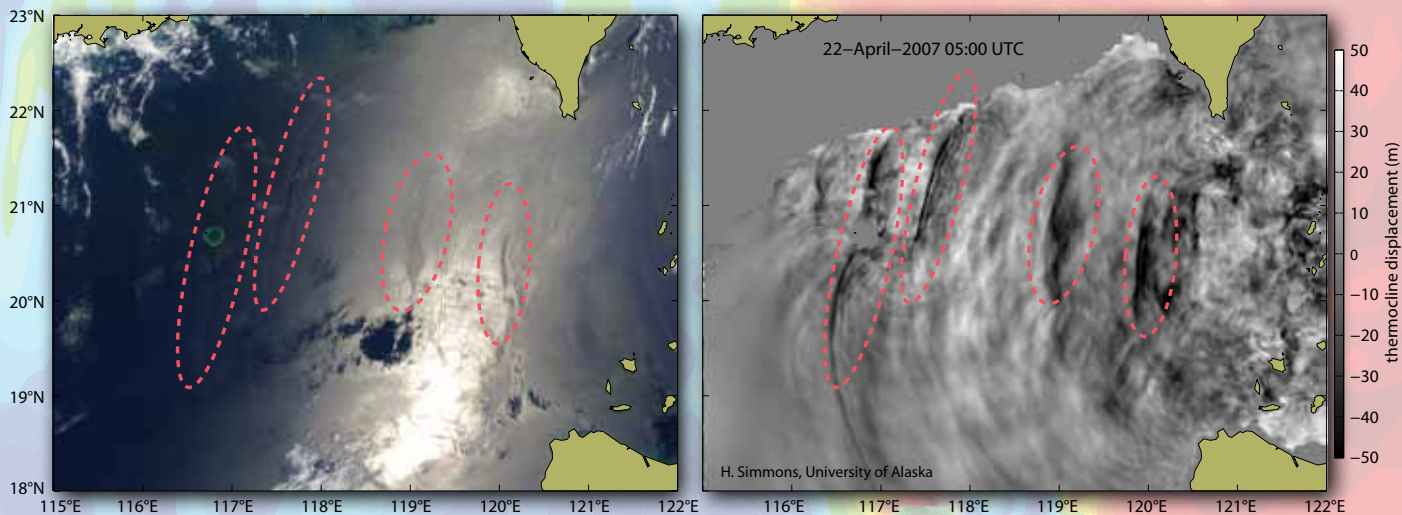
This article has been published in *Oceanography*, Volume 24, Number 4, a quarterly journal of The Oceanography Society. Copyright 2011 by The Oceanography Society. All rights reserved.

USAGE

Permission is granted to copy this article for use in teaching and research. Republication, systematic reproduction, or collective redistribution of any portion of this article by photocopy machine, reposting, or other means is permitted only with the approval of The Oceanography Society. Send all correspondence to: [info@tos.org](mailto:info@tos.org) or The Oceanography Society, PO Box 1931, Rockville, MD 20849-1931, USA.

# Modeling and Prediction of Internal Waves in the South China Sea

BY HARPER SIMMONS, MING-HUEI CHANG, YA-TING CHANG, SHENN-YU CHAO,  
OLIVER FRINGER, CHRISTOPHER R. JACKSON, AND DONG SHAN KO



Comparison between predicted nonlinear wave positions in the South China Sea and those observed by Moderate Resolution Imaging Spectroradiometer (MODIS) April 22 at 5:05 pm. The MODIS image (left) shows sun glint, whereas the simulation (right) indicates deviation of the 200 m isotherm induced by the internal tide and nonlinear internal waves. Red dashed ellipses are at the same locations in both panels, highlighting the corresponding nonlinear wave front positions.

**ABSTRACT.** Nonlinear internal solitary waves generated within Luzon Strait move westward across the northern South China Sea, refract around Dongsha Atoll, and dissipate on the Chinese continental shelf after a journey of over 500 km lasting more than four days. In the last 10 years a great deal of observational, theoretical, and modeling effort has been directed toward understanding and predicting these solitary waves and their effects on the oceanography of the northern South China Sea. This paper reviews a variety of modeling approaches (two- and three-dimensional, kinematic, hydrostatic, and nonhydrostatic) that have been employed to gain insight into the generation mechanisms and physics of the South China Sea's nonlinear solitary waves with the goal of predicting wave characteristics such as phase speed, amplitude, and arrival time.

## INTRODUCTION

The deep basin of the South China Sea (SCS) is the largest marginal sea in the tropics. Luzon Strait, comprised of the Heng-Chun and Lan-Yu Ridges that run north-south between the islands of Luzon and Taiwan, connects the SCS and the Pacific Ocean (Figure 1). Semidiurnal and diurnal barotropic tidal currents with magnitudes reaching  $100 \text{ cm s}^{-1}$  during spring tides flow nearly east-west across the ridge topography. The coincidence of a strong but shallow thermocline in Luzon Strait and large tidal currents results in the generation of large-amplitude internal waves of tidal frequency (internal tides) that radiate away from Luzon Strait into both the South China Sea and the western Pacific. The westward-propagating tides steepen and evolve into large-amplitude nonlinear internal waves that can be identified in satellite imagery and in situ observations (Figure 2 and Farmer et al., 2011, in this issue).

Observations indicate that the internal solitary waves in the South China Sea region are among the largest and fastest in the world, with wave amplitudes in excess of 100 m and propagation speeds close to  $3 \text{ m s}^{-1}$  (Klymak et al., 2006;

Alford et al., 2010). The waves occur regularly between March and November and intermittently from December to February. Their surface expressions can include bands of rough whitecaps of up to 2 km or more in width with along-crest lengths of several hundred kilometers (figure opposite and Figure 3).

In recent years, modeling and field programs have become ever more tightly integrated as modeling capabilities have continued to improve. Studies of internal

tides within a few wavelengths of their generation site are uniquely suited to simulation because the basic physics is controlled by the boundary conditions of the deterministic and episodic tidal forcing and bathymetry. An example of this combined approach is the three-dimensional tide modeling that was integrated into the Hawaiian Ocean Mixing Experiment (HOME; Merrifield and Holloway, 2002). This concept of model/data synergy has been applied over the 11 years of observational programs in the South China Sea, where multiple modeling efforts have been pursued to understand the smaller-scale internal wave features, with the ultimate goal of predicting their generation times and physical characteristics. The modeling work has been at the leading edge in its goal of predicting, to within one hour or less, the arrival time of a phenomenon (internal waves) with cross-wave spatial scales of kilometers

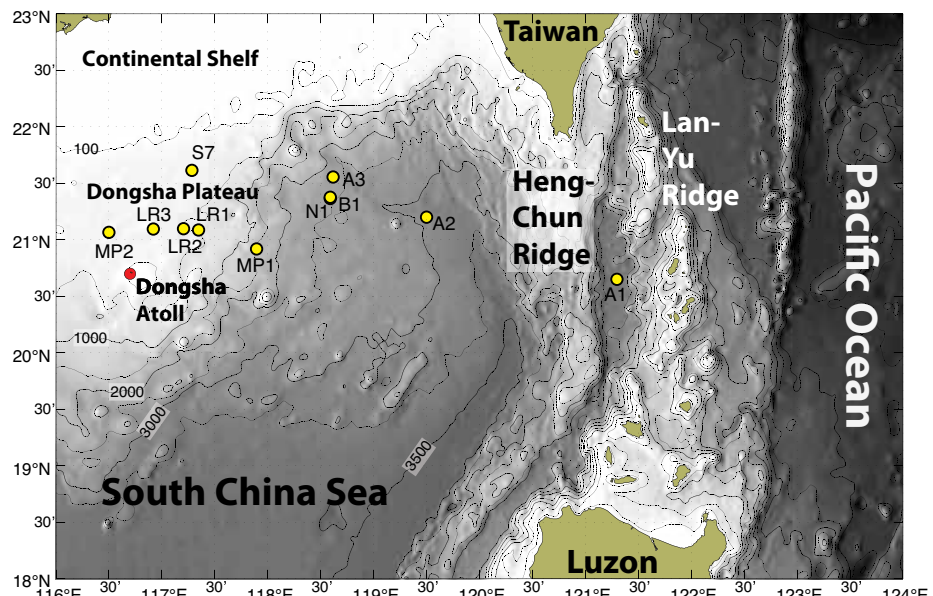


Figure 1. Location map of Luzon Strait between the islands of Taiwan and Luzon, and the Heng-Chun and Lan-Yu ridge systems within it. The yellow dots are moorings referenced in the text.

or less moving swiftly in a domain with a spatial extent of hundreds of kilometers. The success of the South China Sea modeling and prediction effort offers a concrete example of the ways in which a suite of models can be used to support observational programs.

Since 2000, numerous international groups, in partnership with the National Science Council of Taiwan, have sponsored a series of programs to collect satellite, ship, drifter, autonomous vehicle, and mooring measurements of the internal solitary waves and the overall oceanography of the northern South China Sea. This

paper reviews a variety of modeling approaches employed to gain insight into the generation mechanism and physics of the nonlinear solitary waves. First, we present an overview of the relevant field programs in the South China Sea and the role of modeling and its increasing integration into those studies. Following the overview, we provide a more detailed description of the modeling approaches along with a summary of their key findings and how they have contributed to both the prediction effort and understanding the generation, radiation, and dissipation physics.

## SOUTH CHINA SEA NONLINEAR SOLITARY WAVE OBSERVATION PROGRAM HISTORY

Some of the first dedicated work focusing on the oceanography in the region northeast of Dongsha Atoll took place in 2000 and 2001 as part of the Asian Seas International Acoustics Experiment (ASIAEX; see, for example, Lynch et al., 2004; Ramp et al., 2004). While the focus of ASIAEX was primarily on acoustics (i.e., how is sound transmission in the ocean affected by the presence of nonlinear solitary waves?), it required a major cross-disciplinary effort involving in situ oceanographic sampling and satellite imaging to characterize the propagation environment and identify the location and extent of the internal waves. One of the major findings of ASIAEX from the physical oceanography standpoint was the identification of a marked regularity of the arrival of nonlinear waves at moorings sites. Ramp et al. (2004) classified the arrivals into two types: “A-waves,” which arrive at the same location at roughly the same time every day, and “B-waves,” which arrive at the same location roughly

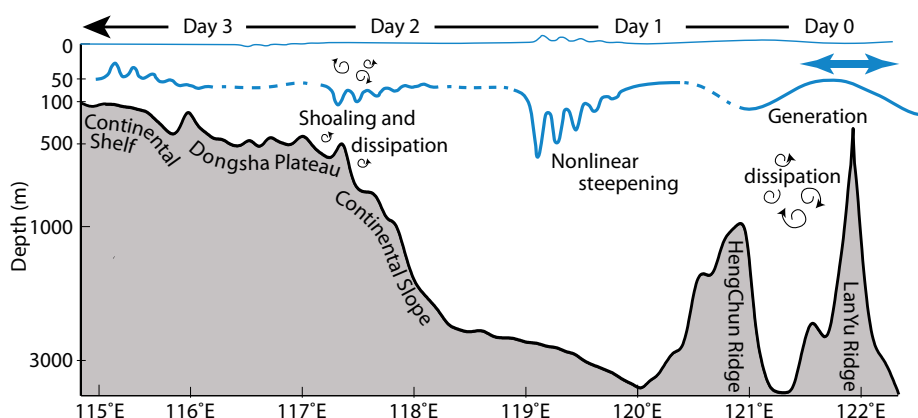
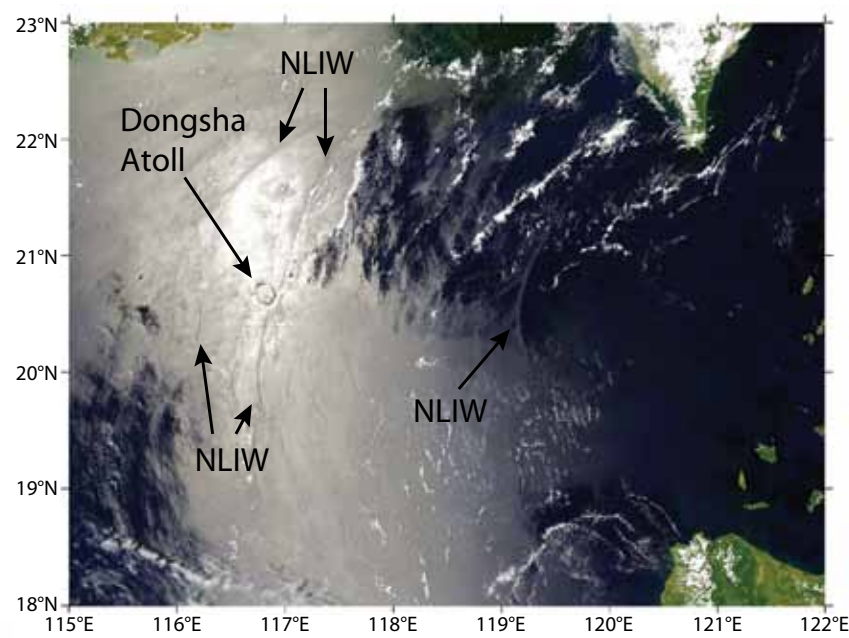


**Figure 2.** Schematic illustrating the generation of an internal tide and its evolution into a nonlinear wave during its three-day journey across the South China Sea.

**Figure 3.** Moderate Resolution Imaging Spectroradiometer (MODIS) true color image of nonlinear internal waves (NLIW) in the northern South China Sea acquired July 13, 2003, at 5:25 UTC. The nonlinear internal waves are generated within Luzon Strait and propagate westward, refracting around Dongsha Atoll before shoaling on the continental shelf. The currents contained within the nonlinear internal waves alter the roughness of the sea surface, allowing the waves to be observed in satellite imagery.



one hour later each day.

In 2005, ASIAEX was followed by the WISE/VANS experiment. Researchers from the United States conducted WISE (Windy Islands Soliton Experiment), while VANS (Variability Around the Northern South China Sea) involved researchers from Taiwan. In addition to intensive observations, this collaborative experiment acquired a full year of internal wave observations from a series of moorings that stretched from Luzon Strait to the continental shelf over 500 km away. Likewise, during the 2007 NLIWI/SCOPE (Nonlinear Internal Wave Initiative-US/South China Sea Oceanic Processes Experiment–Taiwan), ships, moorings, and satellites acquired additional data on nonlinear waves in the region. Using knowledge of the internal solitary waves obtained from the 2005 WISE/VANS investigations, the NLIWI/SCOPE effort in 2007 had, for the first time, the benefit of first-principles dynamical model-based predictions of nonlinear internal wave arrival times to assist researchers during the main portion of the ship-based studies. Predictions by the Naval Research Laboratory (NRL), the University of Alaska Fairbanks (UAF), and Global Ocean Associates (GOA) were used to plan field experiments (e.g., St. Laurent et al., 2011, and Farmer et al., 2011, in this issue). The characteristics of the UAF, NRL, and GOA prediction systems will be discussed in more detail in the next section, and a summary of internal waves models applied to the South China can be found in Table 1.

NLIWI/SCOPE focused on the far-field signal that arises from nonlinear solitary waves as they transit the South China Sea and shoal upon the continental

shelf in the vicinity of Dongsha Atoll. A desire to further understand the full life cycle of the waves prompted IWISE (Internal Waves in Straits Experiment), a focused study of internal wave generation within Luzon Strait. A pilot program was conducted in 2010, which benefitted from modeling efforts that began in 2005. The resulting predictions, time-average maps of baroclinic conversion, and associated internal wave flux were used for mooring placement and planning of shipboard surveys (Alford et al., 2011; Farmer et al., 2011, in this issue). The main experiment was conducted in summer 2011. Presently, analysis is underway, with numerous modeling groups having offered either regional predictions or process-oriented simulations of generation physics to aid in both the design of the experiment and the scheduled shipboard collections.

To complement the in situ measurements, each of these internal wave observation programs in the South China Sea has had a satellite imagery collection component to help provide a synoptic view of the internal wave activity. Nonlinear internal waves contain currents that produce convergent (rough) and divergent (smooth) regions on the ocean surface that move in phase with the internal wave subsurface crests and

troughs. These rough/smooth regions are distinctive features in satellite imagery of the sea surface and appear as bands of light and dark patterns that form a two-dimensional snapshot at a fixed point in time of the wave positions in the South China Sea. While the in situ measurements acquired during each of the field programs produced data on the nonlinear internal waves with a very high temporal resolution (minutes), these observations are by their nature limited in spatial coverage. Satellite imagery, by contrast, can produce measurements that can cover hundreds of square kilometers at moderate spatial resolution (30 m to 250 m), but useful images may only be available at hourly or daily time intervals.

Such a comprehensive set of in situ and remote-sensing observations has provided the modeling effort with excellent data with which to validate results. Such extensive data, however, give rise to an equally daunting task of simulating the internal wave field fully in three dimensions over a very large region and in high temporal and spatial resolution. The next section summarizes several of the modeling efforts and approaches undertaken as part of the South China Sea nonlinear solitary wave observation programs.

---

**Harper Simmons** ([hlsimmons@alaska.edu](mailto:hlsimmons@alaska.edu)) is Associate Professor, School of Fisheries and Ocean Science, University of Alaska Fairbanks, Fairbanks, AK, USA. **Ming-Huei Chang** is Assistant Professor, Department of Marine Environmental Informatics, National Taiwan Ocean University, Keelung, Taiwan. **Ya-Ting Chang** is PhD Candidate, Institute of Oceanography, National Taiwan University, Taipei, Taiwan. **Shenn-Yu Chao** is Professor of Oceanography, Horn Point Laboratory, University of Maryland Center for Environmental Science, Cambridge, MD, USA. **Oliver Fringer** is Associate Professor, Environmental Fluid Mechanics Laboratory, Department of Civil and Environmental Engineering, Stanford University, Stanford, CA, USA. **Christopher R. Jackson** is Chief Scientist, Global Ocean Associates, Alexandria, VA, USA. **Dong Shan Ko** is Oceanographer, Naval Research Laboratory, Stennis Space Center, MS, USA.

## CLASSES OF PREDICTION SYSTEMS

The complexity of the systems used to predict internal wave arrival time and properties depends on the time and length scales of interest and the desired accuracy. The largest and lowest-frequency scales involve internal tides and associated weakly nonlinear internal waves with wavelengths of tens to hundreds of kilometers; they can be predicted well with simple statistical or kinematic models. These models relate the arrival time of the internal tide at some location in the SCS basin to the barotropic tides in Luzon Strait. If the structure and characteristics of the waves such as the amplitude and velocity field or a physical understanding of the generation and propagation physics is needed, then three-dimensional dynamical models are required. In general, higher resolution is desirable if more physical processes are to be simulated. However, three-dimensional models are computationally intensive.

For example, a three-dimensional model with 1 km horizontal grid resolution and 10 m vertical resolution requires a supercomputer with at least 250 processors running for over a week ( $> 40,000$  CPU-hours) to simulate two weeks of internal waves in the SCS.

Three-dimensional models are typically classified as either hydrostatic or nonhydrostatic. Hydrostatic models are sufficient to predict the behavior of waves that are long relative to the depth of the thermocline (Vitousek and Fringer, 2011). Therefore, hydrostatic models can predict the structure of the linear internal wave field before the internal tide steepens into nonhydrostatic waves with wavelengths commensurate with the depth of the thermocline. In the South China Sea, the wavelength of the internal tide is typically longer than the depth of the thermocline east of the continental slope. West of the continental slope, not only do nonlinear effects induced by the waves themselves lead to further

steepening, but topographic effects also contribute. The combination of these two effects produces complex nonlinear and nonhydrostatic phenomena with horizontal scales that are less than 100 m and are beyond the reach of even the fastest supercomputers if basin-scale simulations are required.

Although predictive capability depends to a great extent on the spatio-temporal scales of interest, the accuracy of the prediction also depends on the accuracy and complexity of the boundary conditions or input parameters. Perhaps the most important aspects of any predictive tool are accurate knowledge of the stratification in the SCS and of the barotropic tides in Luzon Strait, which require detailed knowledge of the bathymetry. The kinematic and three-dimensional models typically assume horizontally uniform stratification, with the exception of the Ocean Nowcast/Forecast System described later. Incorporating the effects of mesoscale circulation and associated

Table 1. Summary of internal wave models discussed in the text. Although not predictive according to our definition, the process studies included in the second half of the table contribute to physical understanding of nonlinear internal waves. Further details can be found in the references.

Model	Geometry	Reference	Type	Predictive/Process
Jackson	2D plan view	Jackson (2009)	Kinematic/empirical	Predictive
RHIMT	3D	Alford et al. (2011)	3D primitive equation, isopycnal coordinates, hydrostatic	Predictive
SUNTANS	3D	Zhang et al. (2011)	3D Navier-Stokes equations, unstructured grid, nonhydrostatic	Predictive
ONFS	3D	Ko et al. (2008b)	Nested, assimilated, 3D primitive equation, hydrostatic	Predictive
POM	3D	Jan et al. (2008)	3D primitive equation, hydrostatic, 9 km resolution	Process
MITgcm	3D	Vlasenko et al. (2010)	Quasi 3D nonhydrostatic, limited domain	Process
Ostrovsky-Hunter	1D, two layer	Li and Farmer (2011)	Analytical/hydrostatic	Process
Nonlinear KdV/MCC	1D, two layer	Helfrich and Grimshaw (2008)	Analytical/nonhydrostatic	Process
ROMS	2D	Buijsman et al. (2010)	2D, sigma coordinate, nonhydrostatic	Process

variability in the stratification, such as that arising from the Kuroshio current on the western boundary of the Pacific Ocean and the eddies that form in the South China Sea, requires a much larger domain or nesting of a three-dimensional SCS-scale model into a mesoscale western Pacific ocean circulation model. Seasonal and synoptic variability in stratification can only be modeled accurately with data assimilation. In what follows, the three-dimensional models are classified according to whether or not they incorporate these larger-scale effects on the stratification.

#### Statistical/Kinematic Models

The regularity in the arrival times of nonlinear solitary waves in the northern South China Sea (Ramp et al., 2004, 2010; Zhao and Alford, 2006; Alford et al., 2010; Farmer et al., 2009) has led to examination of the relationship between the solitary wave generation time and phase of the barotropic tide as the basis for a statistical or kinematic-based prediction model. This kind of modeling approach is two dimensional (in the plane of the ocean surface).

Zhao and Alford (2006) developed a simple arrival-time model that correlated internal wave arrival times as indicated by isotherm depression peaks at shelf moorings (deployed in 2000 and in 2001) with peak westward barotropic tidal currents in Luzon Strait. The model showed that peaks in the westward current lagged the internal wave arrivals by approximately 56 hours, a time that is consistent with the propagation speed of a mode-1 linear internal wave. For 25 internal wave packets observed over 21 days in April 2000, Zhao and Alford (2006) reported an RMS arrival time error of 1.0 hour with a maximum error

of 3.8 hours. Similarly, for 35 internal wave packets observed over 27 days in April and May 2001, RMS error was 0.9 hours with a maximum error of 2.1 hours (Zhao and Alford, 2006). In both cases, the authors assumed a straight-line path between a point-source origin near the Batan Islands (roughly

positions of 141 internal wave signatures inferred from 73 satellite images acquired between April 2003 and December 2006. A total of 304 internal wave events detected at two deepwater moorings between May 2005 and May 2006 were also used. The model produced an RMS error in arrival times

“ THE COMPLEXITY OF THE SYSTEMS  
USED TO PREDICT INTERNAL WAVE ARRIVAL  
TIME AND PROPERTIES DEPENDS ON THE  
TIME AND LENGTH SCALES OF INTEREST AND  
THE DESIRED ACCURACY. ”

halfway between Taiwan and Luzon) and the mooring locations.

A more generalized approach using the same principle as Zhao and Alford (2006) was developed in Jackson (2009). The Jackson (2009) method makes use of the internal wave signatures recorded in satellite imagery to determine the parameters of a model function that relates the internal wave phase speed to depth. By establishing the phase speed of the internal waves over a region of interest, the propagation time and propagation path between an origin and any point in the region can be calculated. Internal wave locations for a particular time since generation can then be represented by contours of propagation time. The parameters of the model function used to define the phase speed are estimated by minimizing the difference between the calculated propagation times and the observed propagation times at wavefronts observed in the imagery.

Jackson (2009) applied his technique to the South China Sea using digitized

of 1.32 hours for solitary waves observed in water depths greater than 1,000 m and 2.55 hours for all depths greater than 200 m. The results are consistent with those of Zhao and Alford (2006). The larger RMS errors for arrival time estimates in depths less than 1,000 m occur because the simple model function of phase speed vs. depth fails to capture the effect of complex oceanographic processes on the slope and shelf that can affect the properties of a nonlinear internal wave.

#### Three-Dimensional Tidal Models

##### *Unstructured-Grid SUNTANS Model*

Zhang et al. (2011) employed the three-dimensional, unstructured-grid, nonhydrostatic SUNTANS model (Stanford Unstructured Nonhydrostatic Terrain-Following Adaptive Navier-Stokes Simulator; Fringer et al., 2006) to understand the dynamics of A- and B-wave formation (Figure 4). The model bathymetry was obtained from the Ocean Data Bank of the National

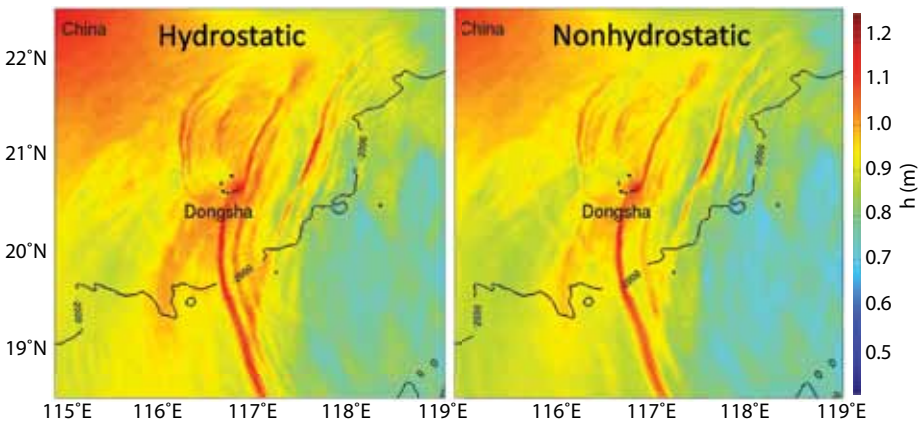


**Figure 4.** Free-surface displacement (in meters above mean sea level) associated with the internal wave signatures at 12:30 am on June 25, 2005, around Dongsha Atoll as computed by the hydrostatic (left) and nonhydrostatic (right) versions of the SUNTANS model.

Center for Ocean Research, Taiwan, with a resolution of 1 arc min (1.8 km). The unstructured nature of the model allowed higher horizontal resolution of 1 km in Luzon Strait, and an average horizontal resolution of roughly 1.5 km throughout the domain shown in Figure 1. The z-level grid employed 100 vertical levels, and the spacing was 10 m near the surface and stretched to 203 m near the bottom. The model is forced at its domain boundaries by the barotropic tides from the TOPEX/POSEIDON (TPXO) 6.2 global tidal model (Egbert and Erofeeva, 2002). The SUNTANS simulations contained 12 million grid cells and took seven days on 64 processors (10,752 cpu hr) to compute a 16-day prediction.

The SUNTANS model accurately predicts the arrival time of the internal waves in relatively deep water (Figure 4). In waters with depths less than roughly 500 m, phase prediction degrades due to the increased dependence on amplitude dispersion and nonhydrostatic effects that are relatively weak in deeper water. This weak amplitude dispersion enables model-predicted phases to be quite good despite inaccurate amplitude prediction.

On average, for small- to moderate-amplitude waves (or 85% of the simulated waves), SUNTANS underpredicts internal wave amplitudes (as measured by deflection of the 15° isotherm) by 30% at moorings B1 and S7 (see Figure 1). This underprediction is generally true for all waves at mooring S7. However, at mooring B1, the predicted wave amplitudes are less than 50% of the observed wave amplitudes. The stark disagreement in amplitude at B1 arises because more accuracy and grid resolution are required to resolve the weakly nonlinear processes that lead to wave steepening and amplitude growth away from topography in the deep SCS basin. This result contrasts with the more strongly nonlinear growth at mooring S7, which is not as sensitive to model accuracy because it is topographically driven.

Despite the inaccurate prediction on the continental shelf, good phase prediction in the deep basin enabled SUNTANS simulations to be used to understand the generation mechanisms and sources of the A- and B-waves observed by Ramp et al. (2010). Fits of circular arcs to the dominant A- and B-wave fronts as indicated by isotherm depression

maps show that the centers of the arcs lie along paths that depend on the type of wave. The centers of the A-wave arcs are aligned with a heading of 282°, while the B-wave arcs are aligned with a heading of 267°. The heading of the A-waves is consistent with the observations of Ramp et al. (2010). Both headings are consistent with the semimajor axes of the tidal ellipses at the eastern of the two ridges in Luzon Strait and imply that A-waves are generated along the ridge to the south of the Batan Islands while B-waves are generated along the ridge to the north. Although the semi-major axes of the diurnal tidal ellipses dominate at the A- and B-wave ridges, the nonlinear features in the SCS are predominantly semidiurnal because diurnal internal tides exhibit excessive rotational dispersion that inhibits nonlinear steepening (Farmer et al., 2009). Along the predominant propagation path of the A-waves, however, deeper topography enables the generation of more semidiurnal internal tidal beams that modulate the westward-propagating semidiurnal internal tide. On the other hand, diurnal beams are relatively weak along the B-wave path in favor of resonance of the semidiurnal internal tide because the spacing between the eastern and western ridges matches the wavelength of the semidiurnal internal tide (Buijsman et al., 2010).

#### RHIMT Isopycnal Model

The University of Alaska RHIMT model (Regional Hallberg Isopycnal Tide Model; Hallberg and Rhines, 1996; Hallberg, 1997) is a regional baroclinic tide model derived from the global Hallberg Isopycnal Tidal Model (HIMT; Simmons et al., 2004). The model has a horizontally uniform stratification taken from near-ridge stratification

from the GDEM (Generalized Digital Environmental Model) hydrographic database (Teague et al., 1990). Model layer thicknesses and densities are designed to optimally resolve the nonlinear waves using WKB (Wentzel-Kramers-Brillouin) stretching, a technique that is standard in internal wave studies (see, for example, Althaus et al., 2003). Tidal currents and elevations from the TPXO global tidal model (Egbert and Erofeeva, 2002) provide the boundary conditions. The model bathymetry is obtained from the 30 arc-second Smith and Sandwell data set. Standard simulations are on a 1/40<sup>th</sup> and 1/80<sup>th</sup> degree horizontal resolution grid (nominally 2.6 km and 1.3 km horizontal resolution, respectively).  $M_2 + S_2 + O_1 + K_1$  predictions at high resolution with both two and 40 layers have been run to cover field programs in 2007, 2008, 2010, and 2011. Lower-resolution experiments have been run for all time periods, with  $M_2$ -only forcing,  $K_1$ -only forcing,  $M_2 + K_1$ , and  $M_2 + S_2 + O_1 + K_1$  tidal constituents, with two and 40 layers.

The 1/40<sup>th</sup> degree configuration has approximately 10 million grid points and requires 15 hours of wall-clock time to run 30 model days on 100 processors (1,500 cpu-hours). This pace is roughly 10 times faster for the same problem size and number of processors than the SUNTANS model, which incurs significant overhead due to solution of the nonhydrostatic pressure. The 1/80<sup>th</sup> degree RHIMT model requires 50 hours of wall-clock time on 250 processors or 12,500 cpu-hours. The advantage of the RHIMT model is that it is computationally inexpensive relative to models such as MITgcm (MIT General Circulation Model; Marshall et al., 1997), ROMS (Regional Ocean Modeling

System; Shchepetkin and McWilliams 2005), or SUNTANS (Fringer et al., 2006), and therefore many test cases or time periods can be run. This advantage is due in part to its isopycnal coordinate configuration that is able to produce a physically meaningful solution with as few as two layers. In fact, the baroclinic structure of the SCS nonlinear internal waves is predominantly mode-1 so that away from regions of direct forcing, a two-layer model is adequate. Forty levels more than adequately resolve the wave structures, the fidelity of which is ultimately limited by horizontal resolution. This computational efficiency allows for a focus on different study periods and isolation of physical processes associated with different tidal constituents. Additionally, the RHIMT model directly

computes barotropic to baroclinic energy transfers and baroclinic energy flux at run time, in a straightforward and accurate manner.

By the metric of occurrence and arrival time of a given nonlinear internal wave event, the 1/40<sup>th</sup> degree resolution model does nearly as well as 1/80<sup>th</sup> degree resolution. However, representation of the generation processes in Luzon Strait is not as accurate at lower resolutions when compared to field data gathered in 2010 (Alford et al., 2011). Figure 5 and the figure on p. 88 demonstrate the model's predictive capability. Like other three-dimensional models, the strength and structure of the predicted waves agree poorly with observations, whereas the model shows skill in prediction of arrival time and

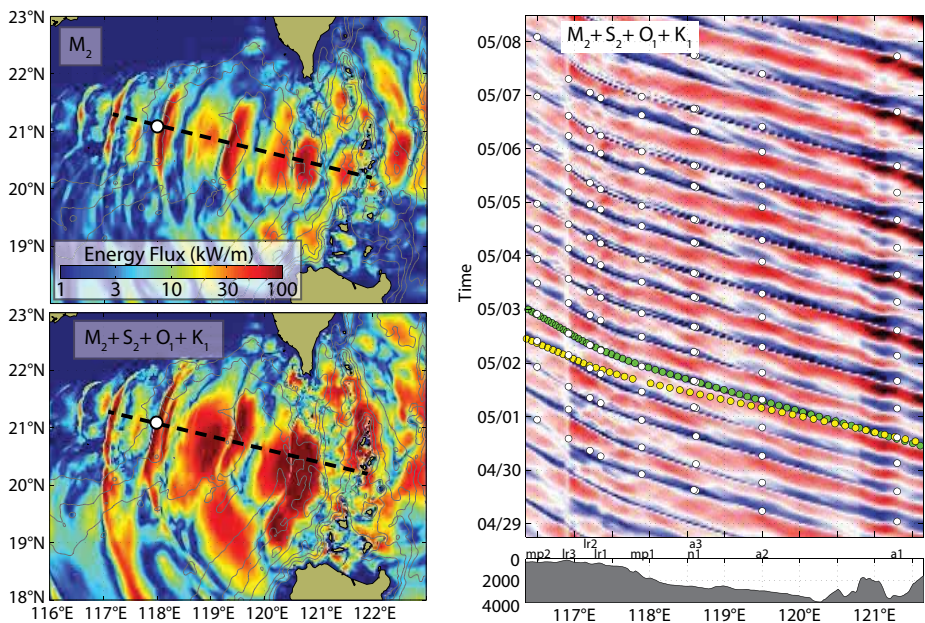


**Figure 5.** RHIMT (Regional Hallberg Isopycnal Coordinate Tide Model) prediction for May 3, 2007, 21:30 UTC. The left panels show depth-integrated internal wave energy flux for experiments forced by the  $M_2$  (top) and  $M_2 + S_2 + O_1 + K_1$  tides (bottom) tides. The white dot shows the location of a nonlinear internal wave that was being sampled by the Taiwanese research vessel *Ocean Researcher 3* on May 4, 2007, 21:30 UTC. The right panel presents the University of Alaska Fairbanks model predicted phase lines showing thermocline displacement (red-white-blue colors) along the line indicated in the panels on the left. White dots are observed wave arrivals deduced from mooring observations (Alford et al., 2010). The moorings are labeled here and in Figure 1. The dense line of green and yellow circles is the mode-1 linear phase speed for  $M_2$  and  $K_1$ , respectively.

location, with RMS arrival time errors of  $1.2 \pm 2.0$  hours (left and right panels of Figure 5). The energy balance from the simulations with four barotropic tidal constituents is as follows: the spring-neap averaged integrated conversion of barotropic to baroclinic tidal energy in Luzon Strait is 35 GW, of which 16 GW and 18 GW are due to diurnal and semi-diurnal waves, respectively. Associated with this is a westward flux of 16 GW integrated across 18–22°N (left panels of Figure 5). Energy radiates away from Luzon Strait at a rate of 26 GW, implying that internal wave energy is lost at a rate of 9 GW in the region.

### Three-Dimensional Assimilative Model

Ko et al. (2008a) used the Naval Research Laboratory Ocean Nowcast/Forecast System (ONFS; Ko et al., 2008b) to predict the propagation of nonlinear internal waves in the South China Sea. Their model is the most comprehensive three-dimensional model of the South China Sea. At its core, the system employs the Navy Coastal Ocean Model (NCOM; Barron et al., 2006), a hybrid vertical-coordinate model that employs both z- and sigma-levels. To simulate nonlinear internal waves in the South China Sea, a 2 km grid is employed in the South China Sea basin. This domain is forced by barotropic tides from the global tidal model OTIS (Oregon State University [OSU] Tidal Inversion Software; Egbert and Erofeeva, 2002), upon which low-frequency, mesoscale currents are superimposed from a coarser 9 km grid model of the entire East China Sea. Both the fine- and coarse-grid models employed 11 sigma layers in the top 149 m of the water column and 29 z layers below. The model

incorporates atmospheric effects via coupling with atmospheric models, and sea surface temperature and height are obtained from satellite data and assimilated into the model in real time.

The multiphysics, nested, assimilative system includes seasonally varying encroachment of the Kuroshio meander from Luzon Strait to the South China Sea (maximal in winter and minimal in summer) and seasonal reversal of mesoscale circulation in the northern South China Sea induced by the East Asia monsoon. Figure 6 shows a prediction of nonlinear internal waves at May 4, 2007, 12:00 UTC, and the model was able to capture the location of nonlinear internal waves reasonably well when compared to the mooring and shipboard observations (Figure 7). However, the predictive accuracy is similar to the

other three-dimensional models because the uncertainty in the larger-scale effects overwhelms their potential role in producing more accurate predictions of internal wave arrival time. This finding is consistent with those of Ramp et al. (2004) who showed that seasonal variability, the Kuroshio intrusion, and mesoscale currents in the SCS incur variability in the arrival time of waves in the western SCS basin by no more than a few hours. Although arrival time is not necessarily predicted more accurately, inclusion of mesoscale currents plays a strong role in modifying the internal wave amplitude. Buijsman et al. (2010) show that the Kuroshio current leads to a thermocline that is shallower on the western side of Luzon Strait than on the eastern side, producing larger-amplitude westward-propagating waves.

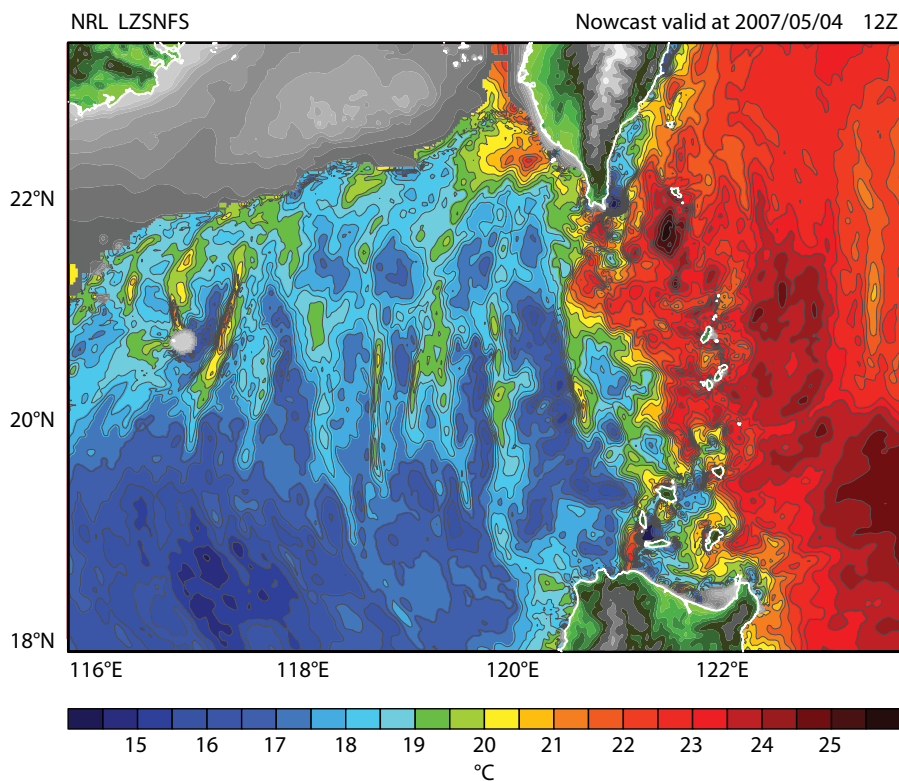


Figure 6. Temperature at 164 m as predicted by the Naval Research Laboratory Ocean Nowcast/Forecast System (ONFS) indicating nonlinear internal depression waves (waves that propagate along near-surface stratification) in the South China Sea.

## TOWARD ACCURATE NON-HYDROSTATIC PREDICTIONS

Although the predictions of Zhang et al. (2011) employ the nonhydrostatic SUNTANS model, the resolution is insufficient to resolve nonhydrostatic effects. Figure 4 illustrates the similarities between the hydrostatic and nonhydrostatic SUNTANS model results. Vitousek and Fringer (2011) derive a criterion for resolution requirements in nonhydrostatic internal wave modeling. They show that accurate resolution of nonhydrostatic effects requires that numerical dispersion induced by model error must be less than the physical dispersion that arises from the nonhydrostatic pressure. For this to occur, the horizontal grid resolution,  $Dx$ , must be less than the effective upper-layer depth,  $h_1$  (i.e.,  $Dx/h_1 = l < 1$ ), where  $l$  is the grid lepticity defined by Scotti and Mitran (2008). In the simulations of Zhang et al. (2011), the average grid lepticity is roughly  $l = (1400 \text{ m})/(200 \text{ m}) = 7$ , which implies that numerical dispersion overwhelms physical dispersion (by a factor of 3.6, following Vitousek and Fringer, 2011), so the dispersion that produces the waves in Figure 5 is mostly numerical. In fact, the dispersion in the nonhydrostatic model is overpredicted because it includes both physical, nonhydrostatic dispersion, and unphysical, numerical dispersion, leading to production of fewer trailing waves in the nonhydrostatic model due to excessive model dispersion. Therefore, in some cases, the hydrostatic result may produce better predictions if the numerical error produces the correct magnitude of the nonhydrostatic dispersion.

Based on the findings of Vitousek and Fringer (2011), the results in Figure 4 have important ramifications for

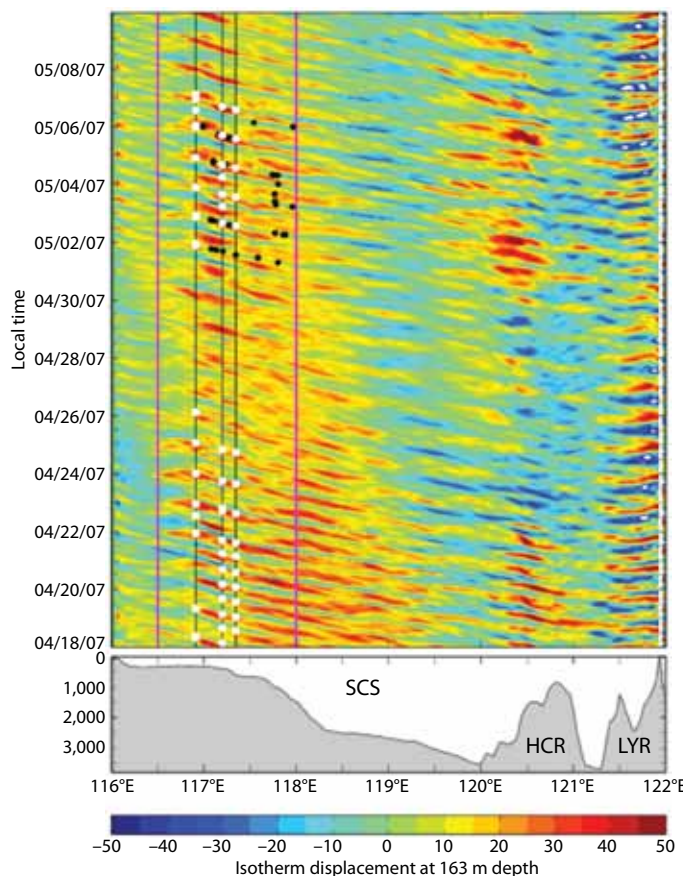


Figure 7. The color contour of the isotherm displacement at 163 m depth along 21°N from ONFS. Predicted nonlinear internal waves are generated at Luzon Strait (122°E) and propagate westward into the South China Sea. The arrivals of the waves indicated by the red color are consistent with observations from three moorings (white circles) and from ship-based observations (black circles). SCS = South China Sea. HCR = Heng-Chun Ridge. LYR = Lan-Yu Ridge.

achieving more accurate internal wave predictions. If the key to accuracy is to minimize numerical dispersion, then accurate simulation of internal waves in the South China Sea requires horizontal grid resolution of  $O(100 \text{ m})$  throughout the domain. This accuracy requires an increase in the number of grid points used by Zhang et al. (2011) in the horizontal by a factor of 50 and increasing the problem size to at least 600 million grid cells. Fortunately, vertical grid resolution is sufficient because it is the large vertical scales (relative to the shortest horizontal scales) that most significantly affect nonhydrostatic dispersion (physical or numerical) in any appreciable way. Although a problem with 600 million grid cells is in principle tractable on modern supercomputers at the Grand Challenge level (requiring

perhaps 10 million CPU-hours), analysis of data from such large simulations is difficult due to the large amount of data involved. It is yet unanswered whether such efforts would lead to substantively better predictions.

## SUMMARY

The northern South China Sea is famously known for its ubiquity of vigorous mesoscale meanders and eddies (Chang et al., 2010). These mesoscale features evolve over timescales of days to weeks or longer, while nonlinear internal waves evolve over timescales of minutes to hours. This disparate ratio of timescales has permitted reasonable forecasts of the location and arrival time of nonlinear internal waves without due consideration to mesoscale circulation. The next level of sophistication in terms

of forecasts must include the mesoscale changes in circulation and stratification, and the ability to forecast the relevant stratification remains the province of the data-assimilating forecast models such as ONFS. For example, the winter reduction of nonlinear internal waves is largely due to the weakening of the thermocline, which arises from changes in mesoscale circulation (Shaw et al., 2009).

The South China Sea has provided a unique laboratory for nonlinear wave predictions. Within this laboratory, the nonlinear internal wave field programs have provided an exceptional opportunity for modelers and observationalists to work together. The fact that different groups have been able to work on the same problem, with ready access to high-quality observations, has lead to significant advances in our understanding of nonlinear waves and our ability to predict their evolution. Dynamical models have proven their ability to predict wave arrivals in the South China Sea from first principles. Confidence in our ability to deploy predictions to as-yet unknown regions has greatly increased.

We have found that certain aspects of the prediction problem are relatively straightforward for a modest computing cluster, with wave arrivals being predictable from first principles. Once waves become highly nonlinear, the details of wave amplitudes and packet structure, for example, are not tractable with hydrostatic, tides-only simulations. The limitations of the models are resolution and knowledge of the bathymetry. Resolution limits simulation fidelity of nonlinear steepening and nonhydrostatic dispersion. Additionally, the turbulent processes of momentum and scalar diffusion are represented with subgrid-scale closure models. Most of the simulations

are restricted to tidal forcing and neglect mesoscale circulation, the presence of the Kuroshio, and seasonal changes in stratification, among other processes. We do not have extensive experience with the ultimate fate of nonlinear waves as they reflect, undergo polarity reversals as they shoal, and ultimately dissipate.

Because the generation of nonlinear internal waves is quasi-deterministic (forced by the tides, shaped by bathymetry, observed within a few wavelengths of their sources), empirical predictions (GOA) or dynamical models (e.g., SUNTANS, RHIMT, ONFS) have proven to be very effective and generally predict wave arrivals in the basin and on the slope to within an accuracy of one to two hours. Although we emphasize the skill of the present generation of models in predicting wave occurrences throughout the basin in waters deeper than 500 m, prediction of packet structure remains elusive. We know that 100 m horizontal resolution at the basin scale, sufficient to accurately simulate nonhydrostatic packet dispersion, presents a computationally expensive but not impossible task for the future. This resolution combined with the as-yet unproven necessity of also including mesoscale dynamics, which would require even greater resources and nesting a nonhydrostatic model within a large-scale data assimilation model, has thus far prohibited comprehensive predictions.

## ACKNOWLEDGMENTS

Harper Simmons gratefully acknowledges the support of the Office of Naval Research (ONR) Young Investigator Program and ONR grants N00014-10-0315 and N00014-05-1-0360 and Robert Hallberg for creating the HIM

model. The Office of Naval Research Physical Oceanography Program supported Christopher Jackson through contract N0001405C0190. Oliver Fringer gratefully acknowledges the Office of Naval Research Young Investigator Program and ONR grants N000140510294, N000141010521, and N000140810904. Shenn-Yu Chao was supported by ONR grant N00014-05-1-0279, Dong-Shan Ko by ONR contract N00014-05WX-2-0647, and Ming-Huei Chang by National Science Council grant NSC98-2745-M-019-00 and ONR grant N00014-04-1-0237. ☐

## REFERENCES

- Alford, M.H., R.C. Lien, H.L. Simmons, J. Klymak, S. Ramp, Y.J. Yang, D. Tang, and M.H. Chang. 2010. Speed and evolution of nonlinear internal waves transiting the South China Sea. *Journal of Physical Oceanography* 40:1,338–1,355, <http://dx.doi.org/10.1175/2010JPO4388.1>.
- Alford, M.H., J.A. Mackinnon, J.D. Nash, H.L. Simmons, A. Pickering, J.M. Klymak, R. Pinkel, O. Sun, L. Rainville, R. Musgrave, and others. 2011. Energy flux and dissipation in Luzon Strait: Two tales of two ridges. *Journal of Physical Oceanography*, <http://dx.doi.org/10.1175/JPO-D-11-073.1>.
- Althaus, A., E. Kunze, and T. Sanford. 2003. Internal tides radiating from Mendocino Escarpment. *Journal of Physical Oceanography* 33:1,510–1,527, [http://dx.doi.org/10.1175/1520-0485\(2003\)033<1510:ITRFME>2.0.CO;2](http://dx.doi.org/10.1175/1520-0485(2003)033<1510:ITRFME>2.0.CO;2).
- Barron, C.N., A.B. Kara, P.J. Martin, R.C. Rhodes, and L.F. Smedstad. 2006. Formulation, implementation and examination of vertical coordinate choices in the global Navy Coastal Ocean Model (NCOM). *Ocean Modelling* 11:347–375, <http://dx.doi.org/10.1016/j.ocemod.2005.01.004>.
- Buijsman, M.C., J.C. McWilliams, and C.R. Jackson. 2010. East-west asymmetry in nonlinear internal waves from Luzon Strait. *Journal of Geophysical Research* 115, C10057, <http://dx.doi.org/10.1029/2009JC006004>.
- Chang, Y.-T., T.Y. Tang, S.-Y. Chao, M.-H. Chang, D.S. Ko, Y.J. Yang, W.-D. Liang, and M.J. McPhaden. 2010. Mooring observations and numerical modeling of thermal structures in the South China Sea. *Journal of Geophysical Research* 115, C10022, <http://dx.doi.org/10.1029/2010JC006293>.

- Egbert, G.D., and S.Y. Erofeeva. 2002. Efficient inverse modeling of barotropic ocean tides. *Journal of Atmospheric and Oceanic Technology* 19:183–204, [http://dx.doi.org/10.1175/1520-0426\(2002\)019<0183:EIMBO>2.0.CO;2](http://dx.doi.org/10.1175/1520-0426(2002)019<0183:EIMBO>2.0.CO;2).
- Farmer, D.M., M.H. Alford, R.-C. Lien, Y.J. Yang, M.-H. Chang, and Q. Li. 2011. From Luzon Strait to Dongsha Plateau: Stages in the life of an internal wave. *Oceanography* 24(4):64–77, <http://dx.doi.org/10.5670/oceanog.2011.95>.
- Farmer, D., Q. Li, and J.-H. Park. 2009. Internal wave observations in the South China Sea: The role of rotation and non-linearity. *Atmosphere-Ocean* 47:267–280, <http://dx.doi.org/10.3137/OC313.2009>.
- Fringer, O.B., M. Gerritsen, and R.L. Street. 2006. An unstructured-grid, finite-volume, nonhydrostatic, parallel coastal ocean simulator. *Ocean Modelling* 14:139–278, <http://dx.doi.org/10.1016/j.ocemod.2006.03.006>.
- Hallberg, R. 1997. Stable split time stepping schemes for large-scale ocean modeling. *Journal of Computational Physics* 135:54–65, <http://dx.doi.org/10.1006/jcph.1997.5734>.
- Hallberg, R., and P. Rhines. 1996. Buoyancy-driven circulation in an ocean basin with isopycnals intersecting the sloping boundary. *Journal of Physical Oceanography* 26:914–940, [http://dx.doi.org/10.1175/1520-0485\(1996\)026<0914:BDCIAO>2.0.CO;2](http://dx.doi.org/10.1175/1520-0485(1996)026<0914:BDCIAO>2.0.CO;2).
- Helfrich, K.R., and R.H.J. Grimshaw. 2008. Nonlinear disintegration of the internal tide. *Journal of Physical Oceanography* 38:686–701, 115, C10022, <http://dx.doi.org/10.1175/2007JPO3826.1>.
- Jackson, C.R. 2009. An empirical model for estimating the geographic location of nonlinear internal solitary waves. *Journal of Atmospheric and Oceanic Technology* 26:2,243–2,255, <http://dx.doi.org/10.1175/2009JTECHO638.1>.
- Jan, S., R. Lien, and C. Ting. 2008. Numerical study of baroclinic tides in Luzon Strait. *Journal of Oceanography* 64:789–802, <http://dx.doi.org/10.1007/s10872-008-0066-5>.
- Klymack, J.M., R. Pinkel, A.K. Liu, and L. David. 2006. Prototypical solitons in the South China Sea. *Geophysical Research Letters* 33, L11607, <http://dx.doi.org/10.1029/2006GL025932>.
- Ko, D.S., P.J. Martin, S.-Y. Chao, P.-T. Shaw, and R.-C. Lien. 2008a. Large-amplitude internal waves in the South China Sea. Pp. 197–200 in *2008 Naval Research Laboratory Review*. Available online at: <http://oai.dtic.mil/oai/oai?verb=getRecord&metadataPrefix=html&identifier=ADA517521> (accessed October 26, 2011).
- Ko, D.S., P.J. Martin, C.D. Rowley, and R.H. Preller. 2008b. A real-time coastal ocean prediction experiment for MREA04. *Journal of Marine Systems* 69:17–28, <http://dx.doi.org/10.1016/j.jmarsys.2007.02.022>.
- Li, Q., and D.M. Farmer. 2011. The generation and evolution of nonlinear internal waves in the deep basin of the South China Sea. *Journal of Physical Oceanography* 41:1,345–1,363, <http://dx.doi.org/10.1175/2011JPO4587.1>.
- Lynch, J.F., S.R. Ramp, C.-S. Chiu, T.Y. Tang, Y.J. Yang, and J.A. Simmen. 2004. Research highlights from the Asian Seas International Acoustics Experiment in the South China Sea. *IEEE Journal of Oceanic Engineering* 29:1,067–1,074, <http://dx.doi.org/10.1109/JOE.2005.843162>.
- Marshall, J., A. Adcroft, C. Hill, L. Perelman, and C. Heisey. 1997. A finite-volume, incompressible Navier Stokes model for studies of the ocean on parallel computers. *Journal of Geophysical Research* 102(C3):5,753–5,766, <http://dx.doi.org/10.1029/96JC02775>.
- Merrifield, M.A., and P. Holloway. 2002. Model estimates of  $M_2$  internal tide energetics at the Hawaiian Ridge. *Journal of Geophysical Research* 107(C8), 3179, <http://dx.doi.org/10.1029/2001JC000996>.
- Ramp, S.R., T.Y. Tang, T.F. Duda, J.F. Lynch, A.K. Liu, C.-S. Chiu, F.L. Bahr, H.-R. Kim, and Y.J. Yang. 2004. Internal solitons in the northeastern South China Sea: Part I. Source and deep water propagation. *IEEE Journal of Oceanic Engineering* 29:1,157–1,181, <http://dx.doi.org/10.1109/JOE.2004.840839>.
- Ramp, S.R., Y.J. Yang, and F.L. Bahr. 2010. Characterizing the nonlinear internal wave climate in the northeastern South China Sea. *Nonlinear Processes Geophysics* 17:481–498, <http://dx.doi.org/10.5194/npg-17-481-2010>.
- Scotti, A., and S. Mitran. 2008. An approximated method for the solution of elliptic problems in thin domains: Application to nonlinear internal waves. *Ocean Modelling* 25:144–153, <http://dx.doi.org/10.1016/j.ocemod.2008.07.005>.
- Shchepetkin, A.F., and J.C. McWilliams. 2005. The Regional Ocean Modeling System: A split-explicit, free-surface, topography following coordinates ocean model. *Ocean Modelling* 9:347–404, <http://dx.doi.org/10.1016/j.ocemod.2004.08.002>.
- Shaw, P.-T., D.S. Ko, and S.-Y. Chao. 2009. Internal solitary waves induced by flow over a ridge: With applications to the northern South China Sea. *Journal of Geophysical Research* 114, C02019, <http://dx.doi.org/10.1029/2008JC005007>.
- St. Laurent, L., H. Simmons, T.Y. Tang, and Y.H. Wang. 2011. Turbulent properties of internal waves in the South China Sea. *Oceanography* 24(4):78–87, <http://dx.doi.org/10.5670/oceanog.2011.97>.
- Teague, W.J., M.J. Carron, and P.J. Hogan. 1990. A comparison between the Generalized Digital Environmental Model and Levitus climatologies. *Journal of Geophysical Research* 95:7,167–7,183.
- Vitousek, S., and O.B. Fringer. 2011. Physical vs. numerical dispersion in nonhydrostatic ocean modeling. *Ocean Modelling* 40:72–86, <http://dx.doi.org/10.1016/j.ocemod.2011.07.002>.
- Vlasenko, V., N. Stashchuk, C. Guo, and X. Chen. 2010. Multimodal structure of baroclinic tides in the South China Sea. *Nonlinear Processes in Geophysics* 17:529–543, <http://dx.doi.org/10.5194/npg-17-529-2010>.
- Zhang, Z., O.B. Fringer, and S.R. Ramp. 2011. Three-dimensional, nonhydrostatic numerical simulation of nonlinear internal wave generation and propagation in the South China Sea. *Journal of Geophysical Research* 116, C05022, <http://dx.doi.org/10.1029/2010JC006424>.
- Zhao, Z., and M.H. Alford. 2006. Source and propagation of nonlinear internal waves in the northeastern South China Sea. *Journal of Geophysical Research* 111, C11012, <http://dx.doi.org/10.1029/2006JC003644>.